

A Predictive Model of Bacterial Foraging by Means of Freely Released Extracellular Enzymes

Y.A. Vetter,¹ J.W. Deming,¹ P.A. Jumars,¹ B.B. Krieger-Brockett²

¹ School of Oceanography, Box 357940, University of Washington, Seattle, WA 98195, USA

² Department of Chemical Engineering, Box 351750, University of Washington, Seattle, WA 98195, USA

Received: 3 June 1997; Accepted: 25 November 1997

A B S T R A C T

Extracellular enzymes are important agents for microbial foraging and material cycling in diverse natural and man-made systems. Their abundance and effects are analyzed empirically on scales much larger than the forager. Here, we use a modelling approach to analyze the potential costs and benefits, to an individual immobile microbe, of freely releasing extracellular enzymes into a fluid-bathed, stable matrix of both inert and food-containing particles. The target environments are marine aggregates and sediments, but the results extend to biofilms, bioreactors, soils, stored foods, teeth, gut contents, and even soft tissues attacked by disease organisms. Model predictions, consistent with macroscopic observations of enzyme activity in laboratory and environmental samples, include: support of significant bacterial growth by cell-free enzymes; preponderance of particle-attached, as opposed to dissolved, cell-free enzymes; solubilization of particulate substrates in excess of resident microbe growth requirements; and constitutive, abundant enzyme release in some environments. Feeding with cell-free enzymes appears to be limited to substrates within a well-defined distance of the enzyme source. Fluxes of dissolved organic material out of pelagic oceanic aggregates and marine sediments, and difficulty detecting dissolved enzymes in such environments, may reflect characteristics of cell-free enzyme foraging and properties of the enzymes. Our calculations further suggest that cell-free enzymes may often be used by microorganisms as the fastest means to search for food.

Introduction

Microorganisms and their extracellular enzymes (EE) are common in many liquid-bathed, natural, and man-made

environments, including pristine and polluted marine and freshwater sediments [3, 6, 69, 79, 87], biofilms [20, 72], stored foods [58], and teeth and soft tissues of organisms [61, 71]. Although microbial enzymes are routinely employed in diverse industrial applications [82], and production of cell-free EE (EE that are actively released from the organism, as opposed to EE that remain associated with the surface of the cell) is commonly enhanced by process engi-

neering [86], constraints on enzyme release in natural environments are not well explored. Despite the ecological, economic, and medical significance of microorganisms and their enzymes, theory and consequent predictions describing cell-free EE production are virtually nonexistent.

Extant quantitative models in microbial ecology have revealed important constraints on chemokinesis [9, 11, 41] and substrate uptake and growth kinetics by bacteria [13] and have identified significant effects of storage allocation [17, 64], body size, temperature, flow regime, and nutrient concentration [43, 45, 49, 52, 89] on microbial growth rates and colony morphologies. These models all considered detection, uptake, transport, and storage of pre-existing dissolved organic material (DOM). Yet, particulate organic material (POM) can be the dominant product of primary production and an important food source for heterotrophic microorganisms in many environments.

Here, we begin development of a quantitative theory of cell-free EE production and associated POM hydrolysis by immobile microorganisms. The strategy is to model costs to the cell in terms of the quantity of EE released and gains by the cell in terms of DOM collected, when DOM is produced by cell-free EE and is derived from POM. The goals are to identify constraints on EE release and POM hydrolysis, and to predict patterns and consequences of microbial feeding with cell-free EE. To do so, we follow the basic premise of optimal foraging theory: i.e., organisms will adopt behaviors, within the range of their abilities, that maximize their net gain rate (gross energy gain rate–energy cost rate). Rather than attempt an all-encompassing theory, we focus these initial efforts on one important class of organisms and environments: Immobile heterotrophic bacteria in aggregates of marine particles and sediments. Much of this derivation may apply to a wider range of microorganisms in diverse settings.

Background

Organic material (OM) is exported downward through the ocean, principally as particle aggregates [28]. Within sediments, most OM remains associated with particles as a layer of organic material sorbed to inorganic sediment grains [50, 57]. Transport of OM into bacterial cells is limited to molecules smaller than about 600 Da by porin size [88]. Heterotrophic bacteria living in particle aggregates and sediments, therefore, must depend largely on extracellular enzymolysis and/or desorption of particulate and particle-sorbed

OM to generate the dissolved, low-molecular-weight compounds required for uptake and metabolism.

The need for extracellular substrate hydrolysis ensures that EE play a key role in microbial ecology and material cycles. Both substrate uptake and bacterial growth may be coupled with extracellular hydrolysis [4, 38, 39]. Bacterial EE can affect partitioning of OM between particulate and dissolved pools in the pelagic ocean [15, 74], and they probably contribute to significant dissolved OM fluxes out of the sediment [12].

Studies with size-fractionated samples [16, 68, 75] and with radiolabelled substrates [37] suggest that cell-attached EE dominate extracellular hydrolysis by free-living marine bacteria, due perhaps to dilution of cell-free EE below detection limits. However, significant dissolved EE activity is sometimes observed in environmental samples [62, 84]; and, for some aquatic and sedimentary environments, cell-free EE are produced by most of the culturable bacteria [42, Vetter unpubl observ]. Although the importance of aquatic EE has long been postulated [34, 54], distinguishing cell-free from cell-attached EE in particle-rich samples remains intractable: Both cell-free EE, which readily adsorb to surfaces, and bacteria (with cell-attached EE) may be predominantly particle-attached.

Nevertheless, cell-free EE-supported bacterial growth and polymer hydrolysis by cell-free EE can be inferred from laboratory and environmental data. In the laboratory, many classic substrate-clearing assays for EE production on agar plates strongly suggest cell-free EE-supported growth. In the environment, most sediment bacteria appear particle-attached and immobile at both pristine and contaminated sites [69, 77, 87]. So do many particle-associated pelagic bacteria [3, 6]. However, many of these attached bacteria (with their cell-attached enzymes) do not directly contact sediment grains [59, 85]. Support of such particle-attached bacteria exclusively by allochthonous DOM (DOM produced by organisms other than the particle-attached bacteria) is conceivable, but inconsistent with the higher activity rates (including EE activity) usually observed for attached, compared to free-living bacteria [29, 48]. For allochthonous DOM feeding, the opposite is expected [33]. Further, because there is sometimes a large DOM flux out of the sediment [12], allochthonous DOM feeding by sediment bacteria would necessitate POM hydrolysis by other benthic organisms. Protozoan and metazoan egestion may release some DOM [44, 60], but bacteria and their EE appear to dominate solubilization and decomposition of particulate detritus [7, 74].

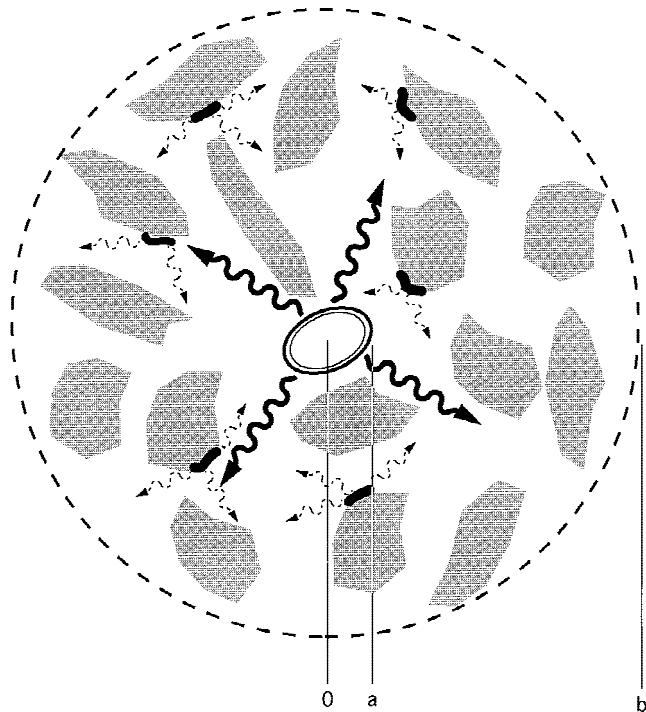


Fig. 1. Particle aggregate (radius b , dashed line) with an immobile, cell-free EE-producing bacterium (radius a , double line) located at the center. The aggregate is composed of impermeable inorganic substratum (shaded polygons) and water-filled pore spaces through which solutes diffuse. Sorbed to the substratum are discrete patches of POM substrate (black shapes). Heavy arrows represent EE diffusing away from the bacterium; dashed arrows, hydrolysate diffusing away from the substrate, where it is produced enzymatically.

Materials and Methods

Model Description: Physical Scenario

The physical scenario modeled is a particle aggregate radius b , with an immobile, cell-free EE-producing bacterium of radius a located at the center (Fig. 1). The aggregate comprises impermeable, inorganic sediment grains (the substratum) and water-filled pore spaces. Sorbed to parts of the substratum surface are discrete patches of POM (the substrate). Substrate remains attached to substratum. Substrate concentration is constant. Hydrolysate is produced by EE acting on substrate throughout the aggregate.

Solute (EE and hydrolysate) movement within the aggregate is by diffusion in the pore water. EE is released at a controlled rate from the surface of the cell. It diffuses outward to the surface of the aggregate, where minimum, background EE concentration is maintained. EE is inactivated at a constant rate. Hydrolysate diffuses either inward, to the surface of the cell, or outward, to the surface of the aggregate. Minimum hydrolysate concentration is maintained at both sites. Solute partition between pore water and particle surfaces. For hydrolysate, a linear relationship between the equilibrium surface concentration and the dissolved hydrolysate

concentration in the adjacent pore water is always assumed. For EE on the substratum, a linear relationship between surface and dissolved concentrations is assumed. For EE on substrate, the equilibrium surface concentration is a saturating function of the EE concentration in the adjacent pore water. The concentration is maximal when a monolayer of enzyme covers the entire surface of the POM. The hydrolysate production rate is linearly proportional to the contact area between active EE and POM.

Mathematical Representation

In a spherically symmetric coordinate system centered on the bacterium, the equations we have developed to describe the enzyme foraging scenario govern both EE concentrations:

$$\frac{\partial}{\partial t} \left[C_e(1 - \psi) + C_e(1 - \delta)\psi\phi k_e + \frac{C_e}{C_e + \frac{1}{k_e\kappa}} \psi\phi\epsilon\delta\gamma \right] = (1 - \psi)D_e \left(\frac{2}{r} \frac{\partial}{\partial r} C_e + \frac{\partial^2}{\partial r^2} C_e \right) - \alpha \left[C_e(1 - \psi) + C_e(1 - \delta)\psi\phi k_e + \frac{C_e}{C_e + \frac{1}{k_e\kappa}} \psi\phi\epsilon\delta\gamma \right] \quad (1)$$

and hydrolysate concentrations:

$$\frac{\partial}{\partial t} [C_h(1 - \psi) + C_h\psi\phi k_h] = (1 - \psi)D_h \left(\frac{2}{r} \frac{\partial}{\partial r} C_h + \frac{\partial^2}{\partial r^2} C_h \right) + \beta \left[\frac{C_e}{C_e + \frac{1}{k_e\kappa}} \psi\phi\epsilon\delta\gamma \right] \quad (2)$$

where C is concentration (of EE or hydrolysate), t is time, and r is radial distance from the origin (the center of the bacterium). Solute currents (flux times area), determined from these equations and other numerical values reported in this text, are calculated using the default (intermediate) values in Table 1, unless otherwise noted.

The left side of the first equation is the rate of change of the average total EE concentration in the aggregate. The first term on the right represents radial diffusion of the EE (in pore water only) of a porous aggregate (see Appendix A). The second term on the right side is the average total EE inactivation rate in the aggregate. The first two terms inside the square brackets are the volumetric EE concentration in liquid and on substratum in the aggregate. The third term inside the brackets is the (saturating) volumetric concentration of substrate-sorbed EE.

The left side of the second equation is the rate of change of the average total hydrolysate concentration in the aggregate. The first term on the right represents radial diffusion of hydrolysate in a porous aggregate. The second term on the right is the total enzymatic hydrolysate production rate in the aggregate.

Steady-state ($\partial/\partial t = 0$) solutions for enzyme and hydrolysate concentrations, and corresponding concentration gradients, were obtained numerically in MATLAB. Boundary conditions for EE

Table 1. Notation and ranges of values used

Symbol	Units	Description	Values ^m
<i>a</i>	cm	Cell radius	1×10^{-5} – 5×10^{-5} – 7.5×10^{-5} ^a
<i>b</i>	cm	Aggregate radius	a – 1×10^{-3} – 1×10^{-2}
<i>C</i>	g cm^{-3}	Pore water concentration of solute	Not a constant
<i>D_e</i>	$\text{cm}^2 \text{s}^{-1}$	Cell-free EE diffusivity	3×10^{-7} – 7×10^{-7} – 1×10^{-6} ^b (MW from 10^4 – 10^6 dalton)
<i>D_h</i>	$\text{cm}^{-2} \text{s}^{-1}$	Hydrolysate diffusivity	1×10^{-6} – 1×10^{-6} – 2×10^{-5} ^b (MW from 10^1 – 10^4 dalton)
EE		Extracellular enzyme	Not a constant
<i>I_{e,a}</i>	g s^{-1}	Diffusion current of cell-free EE from <i>a</i> , ≡ EE release rate by the cell	0 – 1×10^{-17} – 1×10^{-17} ^c
<i>I_{h,a}</i>	g s^{-1}	Diffusion current of hydrolysate to <i>a</i> , ≡ hydrolysate collection rate by the cell	See text
<i>J</i>	$\text{g cm}^{-1} \text{s}^{-1}$	Diffusive flux	Not a constant
<i>k_e</i>	$\frac{\text{g cm}^{-2}}{\text{g cm}^{-3}}$	Equilibrium ratio of substratum-sorbed to pore water-dissolved cell-free EE.	5×10^{-4} – 1×10^{-3} – 5×10^{-3} ^{d,f}
<i>k_h</i>	$\frac{\text{g cm}^{-2}}{\text{g cm}^{-3}}$	Equilibrium ratio of substratum-sorbed to pore water-dissolved hydrolysate	1.3×10^{-3} – 2×10^{-2} – 4×10^{-2} ^{e,f}
<i>r</i>	cm	Radial distance from center of cell	Not a constant
<i>t</i>	s	Time from beginning of EE release	Not a constant
α	s^{-1}	Cell-free EE inactivation coefficient	10^0 – 10^{-3} – 10^{-5} ^g (Half life ~1 s to ~1 d)
β	s^{-1}	Hydrolysate production rate	10^0 – 10^1 – 10^3 ^h
δ	dimensionless	Fraction of particle surface area covered by substrate	0 – 0.1 – 1
ε	dimensionless	Fraction of surface area available to cell-free EE	0 – 0.15 – 0.3 ⁱ (Area in sediment grain pores >15 nm.)
ϕ	$\text{cm}^2 \text{cm}^3$	Ratio of particle surface area to particle volume	1.8×10^4 – 9×10^5 – 1.8×10^6 ^j
γ	g cm^{-2}	Monolayer density of substrate-sorbed EE	1×10^{-6} – 5×10^{-6} – 1×10^{-5} ^k
κ	$\text{cm}^2 \text{g}$	Factor by which affinity of cell-free EE for substrate exceeds affinity for substratum; May also be viewed as increase in effective equilibrium constant for binding of cell-free EE to substrate as compared to substratum at low cell-free EE concentration	1 – 10 – 100 ^k
ψ	dimensionless	Fraction of volume occupied by particles	0.01 – 0.5 – 0.7

^a Size ranges for attached bacteria in [1, 14, 36, 65]

^b Based on molecular-weight data in [18, 31, 46] and diffusivities in [22]

^c Maximal values for a rapidly growing bacterium producing cell-free EE, not 'typical' marine bacteria as with other constants. Based on 2×10^{-14} g C bacterium⁻¹, doubling time of 3 h, growth efficiency of 10% and comparable rates of EE release and biomass increase. Maximum is used as default based on predicted EE release rate pattern (see text).

^d Based on ratios of substratum-sorbed to dissolved EE activities measured in sterile suspensions of substratum particles in artificial seawater medium (Vetter and Deming, unpub). EE activity was added to sterile particle suspensions as cell-free supernatants prepared from pure cultures of marine sediment bacteria grown in artificial seawater medium using chitin or amylopectin as a carbon source. EE activities measured and substrata used were chitinase on amylopectin and amylase on chitin. Activity was measured with internal standards on aliquots of whole and liquid-only (particle-free) fractions of the suspension using fluorogenic substrate analogs (4-methylumbelliferyl N-acetyl- β -D-glucosaminide and 4-methylumbelliferyl α -D-glucoside). Activity was assumed proportional to enzyme concentration and normalized substratum surface areas measured by N₂ adsorption. Due to the use of organic particles as the substratum, the *k_e* values reported here may somewhat overestimate in situ values for EE on inorganic sediment grains.

^e Based on pore-water dissolved OC concentrations in [10, 12, 35], on total sediment organic material content of 1 to 3 %, on surface area:mass data in [56] and on sediment density of 1.5 g cm^{-3} [25]

^f These coefficients are controlled both by the affinity of the solute for the surface (the numerator of the ratio [sorbed concentration]/[dissolved concentration]) and the inherent solubility of the solute in the pore water (the denominator of this ratio). We suspect differences between *k_e* and *k_h* are driven primarily by changes in the affinity (see footnote l).

^g Few data on in situ enzyme lifetimes are available. Although lifetimes of cell-free EE may reach weeks in vitro [32], time course analyses of dissolved EE in seawater [48] suggest that in situ lifetimes are unlikely to exceed a few hours.

^h From Table 10.2 in [55]

ⁱ Based on width distribution data for grain pores in continental shelf sediments in [56] and on enzyme maximal linear dimension of 10 nm

^j Based on surface area:mass data in [56] assuming sediment mineral density of 3.5 g cm^3 [25]

^k Based on an enzyme molecule 10 nm \times 5 nm bound to substrate over 10% of its area

^l Increased specificity of enzyme-substrate as compared to enzyme-substratum binding has long been exploited in affinity chromatography for purification of enzymes and may be due to specific, non-catalytic substrate binding domains, such as for glycogenase, or in the case of multi-protein enzymatic complexes, to separate substrate-binding proteins, such as for cellulase. Data obtained as described in footnote (d) above but for chitinase activity on chitin and cellulase activity on cellulose indicate that coefficients for binding to substrate exceed those for binding to substratum by at least one to two orders of magnitude.

^m Values listed in order from lowest to default (intermediate) to highest values

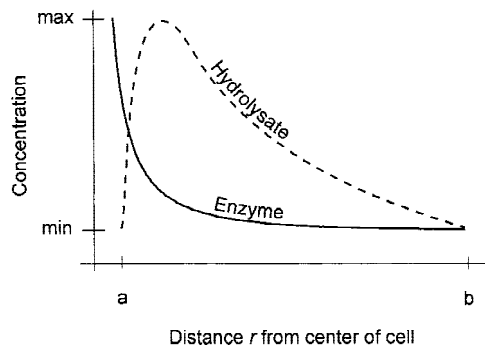


Fig. 2. Schematic representation of EE and hydrolysate concentrations around the bacterial cell. Solid line is the enzyme concentration; dashed line, the hydrolysate concentration. a and b as in Fig. 1.

concentration were the (continuous) EE flux from the cell (at a) and the (constant, minimum) EE concentration at the periphery of the aggregate (at b). Boundary conditions for hydrolysate were the (constant, minimum) hydrolysate concentration at the cell surface and at the periphery of the aggregate.

Numerical solutions for enzyme and hydrolysate concentrations were checked by comparing with analytical solutions, wherever possible. In the limit case of low (non-saturating) EE concentrations and zero inactivation of EE, steady-state numerical and time-dependent analytical solutions (see Appendix B, equation A2) approached the same value after short intervals (seconds to minutes); for low enzyme concentration with inactivation of EE, steady-state numerical and analytical solutions (see Appendix B, equation A3) gave the same result.

The EE maximum is always at a , with concentration and magnitude of the gradient decreasing towards b . The hydrolysate concentration maximum always lies between a and b (Fig. 2). Total hydrolysate currents were determined using calculated concentrations:

$$I_{h,r} = 4\pi r^2(1 - \psi) \left(-D_h \frac{\partial}{\partial r} C_h \right) \quad (3)$$

The hydrolysate current to the cell ($I_{h,a}$) from within b was calculated from the concentration gradient at a ; the hydrolysate current out of the aggregate ($I_{h,b}$) from the gradient at b . The hydrolysate collected by the cell from only the portion of the aggregate within $a < r < b$ was calculated by reducing the enzymatic hydrolysis rate to zero outside r .

Model Design and Assumptions

Hydrolysate currents and other model outputs are dependent on the values used for the necessary constants (Table 1). Many values are poorly constrained: Because the specific organisms and environments manifesting cell-free EE have mostly resisted empirical

identification, particular values appropriate to cell-free EE feeding are unknown. We have, therefore, used values spanning the range of published data from all marine environments. As a baseline, we identify a default, usually intermediate, value for each constant (Table 1).

We refer to bacteria and sediments that correspond to the constant default values as 'typical'. Throughout this work, we identify both a range of model outputs and the output for 'typical' bacteria and sediments. Whereas global marine data were used to determine default constants, oceanic settings in which bacteria feed with cell-free EE are more limited. Corresponding values of constants may lie far from global intermediates. It would, therefore, be incorrect to interpret outputs for 'typical' bacteria and sediments to reflect mean values for systems in which bacteria feed using cell-free EE.

The model was kept as simple as possible while retaining the essential features of cell-free enzyme foraging, and providing a conservative estimate of hydrolysate collection rates by the bacterium. Our aim is to identify specific features of particle aggregates, solutes, and microbes that constrain cell-free foraging, without losing general relevance across the differing (mostly under-characterized) environments in which foraging with cell-free EE may be a viable feeding mechanism. This goal led to specific model assumptions. The common thread binding them is the primary constraint of solute transport by diffusion in pore water.

We postulated a single, idealized forager at the center of the aggregate. A mutualistic consortium of organisms engaged in co-ordinated foraging could reap increased overall benefits, while the presence of competitive strains or assemblages might reduce them. Similarly, micrograzers could have significant and diverse impacts, both by reducing bacterial populations and by releasing intracellular enzymes. However, possible organism types, distributions and activities in the environment are numerous. At this stage in developing theory on microbial EE, little empirical information is available on the juxtaposition of physiological types that could provide focus.

We considered enzymatic foraging on an uncharacterized particulate carbon source. Foraging with non-enzyme solutes such as surfactants may also be an important feeding strategy, and we recognize that the type of substrate (e.g. protein vs. carbohydrate) strongly influences microbial ecology. By modeling generic solute transport, we hope to maintain relevance to a diversity of solutes, substrates, and microorganisms. Considering particulate substrates necessitates two-way transport (EE to substrate, hydrolysate to bacterium), ensuring conservative estimates of benefits.

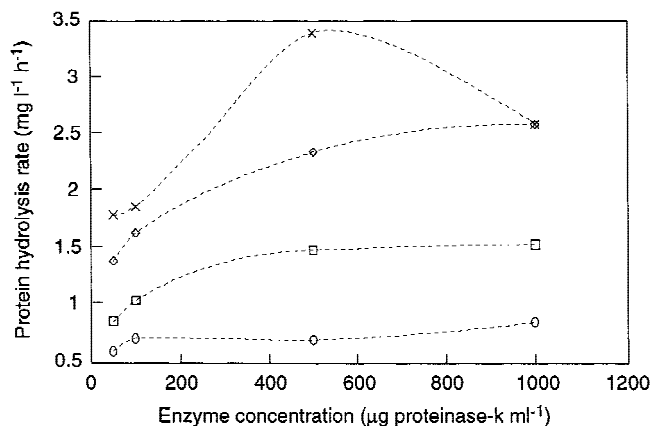
We excluded effects of enclosure. This exclusion is reasonable for the high porosities characteristic of many pelagic aggregates, and the top few centimeters of sediments that also support significant microbial activity rates [24, 78]. Mass transfer by diffusion in the pore space is relatively insensitive to the impermeable phase; molecular mean free paths are still long, relative to characteristic pore dimensions.

We disregarded solute transport by pore-water advection due to compaction, pumping or settling [76]. This is justified for most situations by calculating characteristic velocities required to pro-

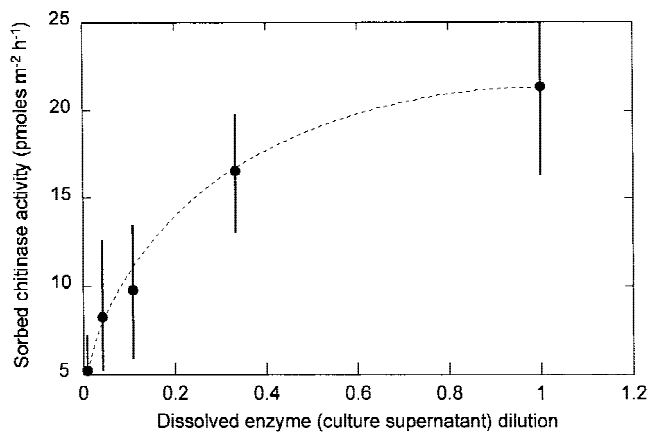
duce Peclet numbers (Pe) >1 for organism dimensions and diffusivities in Table 1. Pe describes the relative importance of advection and diffusion to solute transport, where numbers >1 indicate advection is the dominant process (see [49] for a description of Pe and its calculation). The necessary characteristic velocities, which exceed 10^{-2} cm s^{-1} , are comparable to or exceed sinking rates of marine fecal pellets [73]. Thus, although advection may be important for bacteria near aggregate boundaries and for microbial consortia (for which foraging length scales may be longer), diffusion probably dominates mass transport within aggregates and in sediments. Chemical gradients within sediments and sinking aggregates are also consistent with diffusion-limited solute transport [1].

We postulated inexhaustible substrate and used steady-state diffusion equations. These apparently gross simplifications are probably justified in many environments. This assertion can be tested by comparing the rate at which solute concentrations stabilize around an immobile cell with the rate at which substrate is consumed. We predicted that EE concentrations often stabilize in only seconds to minutes (Fig. 3); hydrolysate concentrations should stabilize at least as quickly, due to higher expected diffusivities (Table 1). Substrate is consumed in hours or more, considerably longer than our time scales (see Appendix C). When EE concentrations stabilize slowly or substrate concentrations are low, the assumptions of inexhaustible substrate and use of steady-state diffusion equations may not be justified. The governing equations, however, can still be useful. Substrate resupply may often be affected on short time scales by coagulation in the water column and sediment transport on the sea floor.

We modeled hydrolysate production rates to saturate with increasing dissolved EE concentration. Use of saturating kinetics is supported by data obtained from experiments using real sediments



A



B

Fig. 4. Hydrolysis rate due to proteinase-k, added at various concentrations, to sediments (A). Data values were obtained by manual measurement of Fig. 5 in Mayer et al. [57]. Curves correspond to initial rate (upper curve) and rates after 15, 30, and 60 min (lower curves). Chitinase activity (B) sorbed to chitin as a function of chitinase dilution (Vetter and Deming, unpublished). Cell-free culture supernatant was prepared from a chitinase-producing marine bacterium. Serial dilutions of the supernatant were added to suspensions of purified chitin. Chitinase activity was measured in dissolved and chitin-sorbed phases of the suspensions, using a fluorescent substrate analog (methylumbelliferyl n-acetyl-glucosaminide). Chitin-sorbed activity was normalized to chitin surface area measured by nitrogen adsorption. Error bars are 90% confidence intervals of replicate samples.

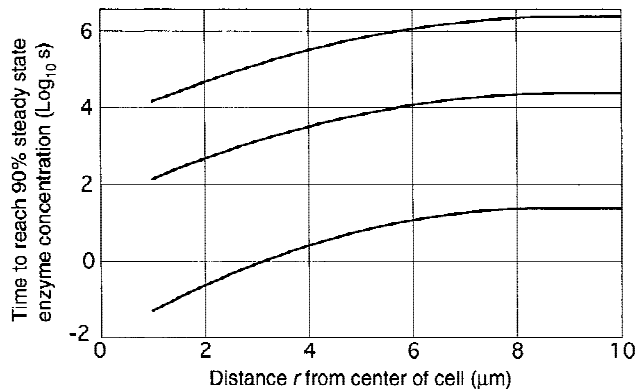


Fig. 3. Times for enzyme concentration to reach 90% of steady-state value, calculated using eq A2 and default constant values (intermediate curve) or constant values producing fastest (lower curve) or slowest (upper curve) approach to steady state.

and commercial enzyme preparations (Fig. 4a, [57]), and artificial substrates and bacterial cell-free EE (Fig. 4b, [26]). Use of the Langmuir isotherm to describe saturation as a consequence of monolayer adsorption of EE is consistent with these data, and reflects the idea that only EE that touches substrate will produce hydrolysate.

Results and Discussion

Hydrolysate Current to the Cell: Effects of Constants

The total current of hydrolysate that returns to a bacterium ($I_{h,a}$) as a result of the current of EE it released ($I_{e,a}$) is the

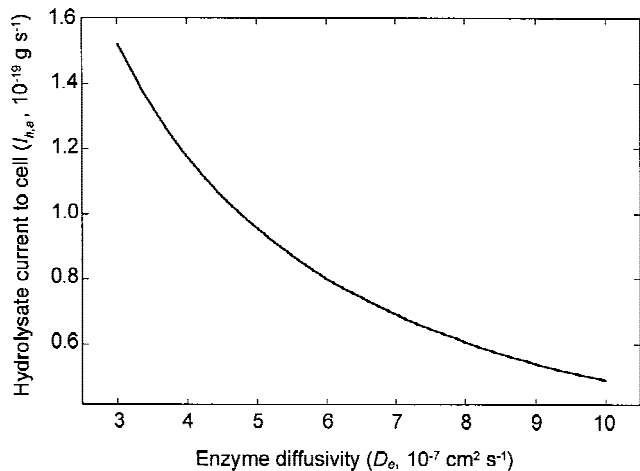


Fig. 5. Hydrolysate current to the cell ($I_{h,a}$) as a function of enzyme diffusivity (D_e). Data generated with all other constants set to default values.

most obvious measure of the benefit of cell-free EE production to the organism. Most of the constants in eqs. 1 and 2 represent bacterial or environmental parameters that affect $I_{h,a}$. Parameters that decrease movement of EE away from the cell or increase the volumetric rate of hydrolysate production increase $I_{h,a}$. Sensitivity to the effect of each constant is revealed as the change in $I_{h,a}$ produced by a change in the constant value (e.g., Fig. 5). Because of interactions between constants, a range of plots may be obtained (not shown); unless the plot is linear, the effect on $I_{h,a}$ may vary. The effect of each constant, *const*, on $I_{h,a}$ is summarized as its median relative effect, $\Delta_{I_{h,a},const}$. With all other constants fixed, $\Delta_{I_{h,a},const}$ is determined by calculating $I_{h,a}$ over the full range of *const* and dividing the ratio (maximum $I_{h,a}$)/(minimum $I_{h,a}$) by the ratio (maximum value *const*)/(minimum value *const*).

These unusual sensitivity coefficients are useful for comparing the effects of constants in the specific physical situations that we consider. Most constants have effects on $I_{h,a}$ of similar magnitude (Table 2). Hence, the property or properties of bacterium or environment with greatest potential influence on $I_{h,a}$ (and consequently on the efficacy of cell-free EE feeding) may shift as the ranges of constant values change across particular organisms and locations.

Hydrolysate Current: Range and Consequences

Because of metabolic costs associated with the production of EE and their subsequent release from a bacterium, we assume that energy accrued from one mass unit of hydrolysate is approximately 10% of the energy lost in producing and

Table 2. Relative effect of constants on hydrolysate flux to the bacterium ($\Delta_{I_{h,a}}$) and on excess solubilization (Δ_{sol})

Constant	Control ^a	$\Delta_{I_{h,a}}$	Δ_{sol}	Bias
<i>a</i>	org	-0.4 ^b , 1, 1	-1.1, -1.1, -1.1	low
<i>b</i>	env	0.6, 0.8, 2	2.5, 0.8, 0.2	low
D_e	org	-0.1, -0.8, -0.2	0.6, 0.9, 0.3	low
D_h	org	0, 0, 0	0, 0, 0	none
I_e	org	1, 1, 1	0, 0, 0	none
k_e	org/env	1, 0.8, 0.2	0, -0.1, -0.4	low
k_h	env	0, 0, 0	0, 0, 0	none
α	org/env	0, 0, -0.4	0, -0.4, -0.9	low
β	org/env	1, 1, 1	0, 0, 0	none
δ^c	env	1, 1, 6	0, 0, 0.5	high
ε^c	org/env	1, 1, 0.3	0, 0, -0.4	low
ϕ	env	1, 0.7, 0.2	0, 0.2, -0.4	low
γ	org	1, 1, 0.3	0, 0, -0.4	low
κ	org	1, 1, 1	0, 0, 0	none
ψ	env	10, 8, 1	0, -0.1, -1.2	high ^d

^a 'Control' indicates whether the constant value is expected to be controlled principally by the organismal ('org') or environmental ('env') factors, or by both ('cell/org'). 'Bias' indicates whether the effect on $I_{h,a}$ and on excess solubilization is greater at low or high constant values. For each constant, ranges of values for $\Delta_{I_{h,a}}$ and Δ_{sol} are obtained by setting all other constants to values that either minimize (first values) or maximize (last values) $I_{h,a}$. Default values for $\Delta_{I_{h,a}}$ and Δ_{sol} (middle values) are obtained by setting all other constants to their default values. All values rounded to nearest 0.1. Negative values indicate an inverse relationship.

^b Negative values of $\Delta_{I_{h,a},a}$ (i.e. -0.4 above for $\Delta_{I_{h,a},a}$ with minimized $I_{h,a}$) result when the bacterial volume is a significant fraction of the total aggregate volume (when *a* is very close to *b*).

^c $\Delta_{I_{h,a}}$ and Δ_{hyp} calculated with minimum constant value equal to 1% maximum value to avoid division by zero

^d Bias shifts from high to low for $\Delta_{sol,bi}$ with maximized $I_{h,a}$.

releasing one unit of EE (see Appendix D). We therefore expect cell-free EE production to be a net benefit primarily when $I_{h,a}$ exceeds $I_{e,a}$ by at least a factor of 10. When $I_{h,a}$ includes a limiting nutrient, such as iron returned by siderophores released from free-living, water-column bacteria [83], this factor may decrease significantly.

The range of predicted hydrolysate currents that might return to a bacterium producing cell-free EE is large (Fig. 6). At default values of the constants, $I_{h,a}$ is two to three orders of magnitude less than the current of enzyme released by the cell ($I_{e,a}$); at extreme values, $I_{h,a}$ may exceed $I_{e,a}$ by five or more orders of magnitude. This suggests that, although feeding with cell-free EE will not always benefit 'typical' marine sediment bacteria (not surprising, because most sediment bacteria appear not to be actively growing [24]), it may sometimes be a powerful mechanism.

Important for interpretation of $I_{h,a}$ is the distinction between constants that can be controlled by the organism (and may be optimized by cell-free EE-producing bacteria) and

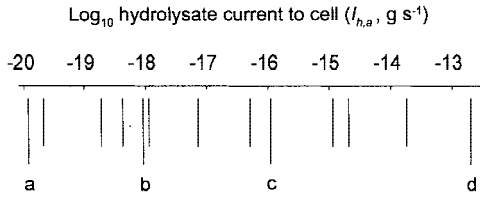


Fig. 6. Hydrolysate current to the cell ($I_{h,a}$). Lines indicate the current obtained as each constant is changed permanently from the default to the optimal (maximal $I_{h,a}$) value (Tables 1 and 2). Longer lines indicate rates with all constants at default value (line a), cell-controlled constants increased to optimal values (line b), cell-influenced constants also increased to optimal values (line c), and environmental constants also increased to optimal values (line d). Shorter, intermediate lines correspond to successive optimization of each individual constant. In order of ascending $I_{h,a}$ from line a, these are the organism-controlled constants α , δ , D_e , and γ (line b); ascending from line b, the organism-influenced constants β , k_e , and ε (line c); ascending from line c, the environment-controlled constants δ , ϕ , ψ , and b (line d).

those that are principally properties of the abiotic environment (and may limit the net benefit to cell-free EE-producing bacteria). Bacteria probably have principal control of a , $I_{e,a}$, κ , and perhaps D_e and γ (D_h might also be controlled by the organism, but cannot significantly affect net benefit to the cell [Table 2]). Bacteria probably also exert some influence on α , β , and perhaps k_e and ε . The abiotic environment controls ϕ , ψ , δ , b , and perhaps k_h .

Adjusting organism-controlled constants to maximize $I_{h,a}$ ($a = 0.75 \mu\text{m}$, $I_{e,a} = 10^{-17} \text{g s}^{-1}$, $\kappa = 100$, $D_e = 3 \times 10^{-7} \text{cm}^2 \text{s}^{-1}$ and $\gamma = 10^{-5} \text{g cm}^{-2}$) yields a hydrolysate current to the cell of about 10^{-18}g s^{-1} (Fig. 6). The only organism-controlled property that might be further adjusted (beyond the maximum value in Table 1) to increase $I_{h,a}$ is substrate-specific enzyme binding, κ (a , $I_{e,a}$, D_e , and γ are too well-constrained). The factor, however, by which it must be increased to yield net benefit is large (at least two orders of magnitude; Table 2). Net benefit from cell-free EE feeding may be difficult to achieve in 'typical' marine sediments if only organism-controlled properties are adjusted.

Adjusting organism-influenced constants, as well, to maximize $I_{h,a}$ ($\alpha = 10^{-5} \text{s}^{-1}$, $\beta = 1000 \text{s}^{-1}$, $k_e = 5 \times 10^{-3} \text{cm}$, $\varepsilon = 0.3$) yields a hydrolysate current to the cell of about 10^{-16}g s^{-1} , which is within the range of currents that might yield net benefit. As environment-controlled constants are adjusted ($\phi = 1.8 \times 10^6 \text{cm}^{-1}$, $\psi = 0.7$, $b = 100 \mu\text{m}$), $I_{h,a}$ can increase to over 10^{-13}g s^{-1} (much greater than the maximum possible hydrolysate uptake rate of a bacterial cell). Net benefit from cell-free EE should be achieved easily in

appropriate aggregates or sediment, even with sub-optimal, organism-controlled constants.

Thus, depending on the degree to which cell-influenced constants are affected by the cell, at least one-half to three-quarters of the increase in benefit to the cell is a consequence of environmental parameters (Fig. 6). As indicated, adjusting cell-controlled constants, alone, will often be insufficient to yield net benefit. Taken together, these predictions, based on adjustments of different model constants, suggest that cell-free EE feeding should be common in some environments and nearly or completely absent in others. Ideal environments for cell-free EE feeding, such as those with chemical and physical properties corresponding to optimal values of the constants, should be characterized by large aggregates (large b) composed of small, young (unweathered), tightly packed (large ϕ , ψ) particles (large ε); fresh, abundant OM (large β , γ), and moderate temperatures (large β).

In the ocean, phytodetritus, fresh marine snow, and zooplankton fecal pellets meet most of the criteria for supporting cell-free EE feeding, as may both the egesta of some deposit-feeding organisms and some microzones in sediments. This may help explain the dominance among marine particle-associated bacteria of *Cytophaga*, and other bacteria known to release EE [23], and the abundant production of cell-free EE activity by periphytic marine bacteria [19]. The degree to which cell-free EE actually support bacterial growth in these environments is not known.

Hydrolysate Current: Importance of Specific Enzyme-Substrate Binding and EE Inactivation Rate

Of the organism-controlled constants, substrate-specific enzyme binding (κ) may offer the most powerful and efficient mechanism for increasing the hydrolysate current to the cell. Although the magnitude of ΔI_{ha} for a , $I_{e,a}$, D_e , and γ is sometimes equal to $\Delta I_{ha,\kappa}$ (Table 2), the range over which these four constants may be adjusted is restricted. Bacteria with radii greater than about $1 \mu\text{m}$ are rarely observed in most marine environments; $I_{e,a}$ is expected to remain high (see below); D_e increases only by approximately $1/3$ the power of molecular weight, exacting costs of decreased diffusivity disproportionate with potential gains; and the density of substrate-sorbed enzymes is limited by the minimum protein size necessary for EE activity.

In contrast, no inherent limit on the range of κ is apparent. κ has been measured infrequently, however, despite abundant qualitative evidence of substrate-specific enzyme binding. Limited quantitative data (Table 1, footnote k) in-

dicating that substrate-specific binding can increase substrate-sorbed, cell-free EE concentrations by at least one to two orders of magnitude over the concentration on non-substrate surfaces. This observation is consistent with measurements of tenacious enzyme-substrate binding from allosteric systems, in which binding and catalysis are effected by separate regions of the enzymes (e.g. cellulase) [5, 27, 40].

Of the organism-influenced constants, differences in the enzyme inactivation rate (α) may have the greatest potential to influence hydrolysate current to the bacterium. This sensitivity is due to the relatively large range over which α may vary, because $\Delta_{I_{h,a}}$ is similar to that for β , k_{ev} and ε (Table 2). EE properties affecting α that may be influenced by the bacterium include resistance to proteolysis, such as by extracellular glucanase [32], and adsorption and unfolding on inorganic sediment surfaces [80].

Interactions of κ and α may be important. Enzyme inactivation can be reduced several orders of magnitude by the presence of substrate (e.g., amylase [81]); maintaining EE near substrate (large κ) may thus decrease α . Further, increased $I_{h,a}$ from decreased α may be realized only given large κ , regardless of its effect on α . Reduced α significantly increases $I_{h,a}$ only when the significant loss term for EE is not diffusion, such as when the current of EE out of the aggregate is small compared to the current of enzyme produced by the bacterium. κ decreases diffusive loss of EE by increasing the quantity of substrate-sorbed vs dissolved EE.

As a result of these model findings, we believe that strong substrate binding, degradation resistance, and long in situ lifetimes may be general and often concomitant properties of cell-free EE. In addition to consequences for microbial feeding, this suite of properties may be important for the interpretation of environmental data. Notably, substrate-specific and non-specific substratum binding may provide an explanation for the low levels of dissolved cell-free EE that have often been measured in size-fractionated environmental samples (e.g. [16, 68, 75]). For most circumstances under which cell-free EE foraging is a viable feeding strategy, such as with environmental parameters corresponding to constants between default to high $I_{h,a}$, the majority of *cell-free* EE in the aggregate is sorbed to the surface of substrate and substratum (Fig. 7). Accordingly, differentiating cell-associated from cell-free enzyme activity cannot be accomplished by 0.2- μm filtration, because the particle-sorbed pool of EE captured on the filter includes both cell-associated and cell-free EE. Measurements of κ and α and their relationships with bacterial growth rate are necessary to clarify the role, quantitative significance, and activity site

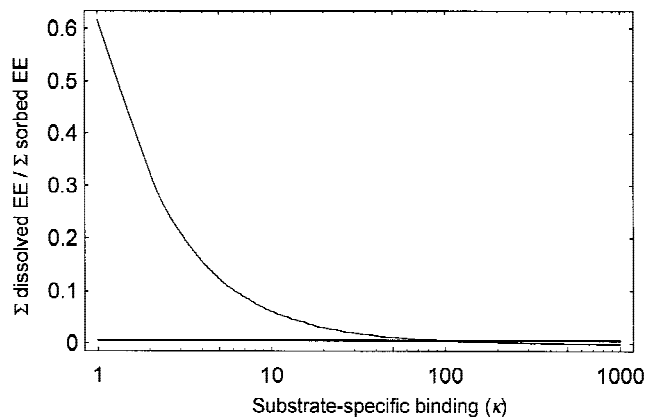


Fig. 7. Ratio of dissolved to sorbed (substratum + substrate) cell-free EE as a function of substrate-specific binding. Data plotted for constants (other than κ ; Table 1) set at values corresponding to maximal $I_{h,a}$ (upper line) and default $I_{h,a}$ (lower line).

of cell-free EE in microbial growth and OM decomposition.

Excess Solubilization: Effects of Constants

Excess solubilization of substratum-sorbed OM is the most obvious biogeochemical effect of cell-free EE feeding. Excess solubilization is the ratio of the hydrolysate current that flows out from the aggregate at b ($I_{h,b}$) to the hydrolysate current collected by the organism at a ($I_{h,a}$). Analogous to $I_{h,a}$, the effect of each constant in eqs. 1 and 2 on excess solubilization is summarized as its median relative effect, Δ_{sol} (Table 2), by calculating $(I_{h,b})/(I_{h,a})$ over the full range of the constant, and dividing the ratio (maximum excess solubilization)/(minimum excess solubilization) by the ratio (maximum constant value)/(minimum constant value). As with $I_{h,a}$, the effect of most constants on excess solubilization is similar (Table 2). No single property of organism or environment is always expected to have a dominant effect on the extent of excess solubilization. All organism-controlled constants have opposite effects on the magnitude of $I_{h,a}$ and excess solubilization.

Excess Solubilization: Range and Consequences

The range of predicted excess solubilization is restricted. The range of predicted $I_{h,a}$ spans at least 7 orders of magnitude; the corresponding range of predicted excess solubilization is narrower, from ~ 6 to 70 (Fig. 8). Optimizing constants (within the range given in Table 2) to increase or decrease

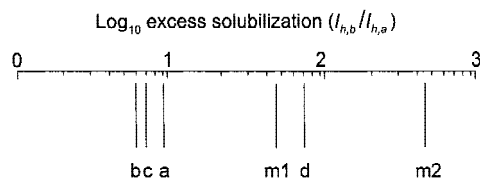


Fig. 8. Excess solubilization of OM accompanying feeding with cell-free EE ($I_{h,b}/I_{h,a}$). Lines a–d indicate excess solubilization corresponding to hydrolysate currents in Fig. 6: all constants at default value (line a); cell-controlled constants increased to optimal values (line b); cell-influenced constants also increased to optimal values (line c); and environmental constants also increased to optimal values (line d). Lines m1 and m2 correspond to constants adjusted for maximal possible excess solubilization in aggregates of radius 10 and 100 μm , respectively. Minimum possible excess solubilization for radius 10 μm aggregate is not significantly different from b.

excess solubilization, rather than $I_{h,a}$, increases the maximum less than 10-fold and does not significantly decrease the minimum. Significantly increasing the range of excess solubilization further, which requires departing from the constant ranges given in Table 2, generally produces $I_{h,a} \ll I_{e,a}$ (data not shown).

We, therefore, believe that cell-free EE feeding by bacteria in particle aggregates usually causes EE excess solubilization (lost hydrolysate) ~one to two orders of magnitude greater than $I_{h,a}$. Achieving quantitative benefit from cell-free EE feeding with much greater excess solubilization is unlikely. Reduced excess solubilization and the associated increased $I_{h,a}$ might be achieved with a mechanism for trapping hydrolysate.

For example, concerted action by microbial consortia or clonal population assemblages could reduce excess solubilization, if bacteria at the periphery of the group acted as passive absorbers, and would also decrease overall (population-averaged) $I_{e,a}$. A somewhat similar division of labor occurs in nitrogen-fixing microbial consortia [63]. Channeling of hydrolysate by exopolymer strands [66] may also serve to reduce (average) excess solubilization in aggregates. Transparent extracellular polysaccharide [1] may be a consequence of microbial mechanisms to trap hydrolysate.

Physical enclosure, within microzones or metazoan guts and their egesta, may also play a crucial role in reducing excess solubilization for some organisms. The same environments expected to support cell-free EE feeding (because of optimal chemical and physical properties supporting high predicted $I_{h,a}$) may also be ideal for trapping hydrolysate. In particular, fecal pellets encased by peritrophic membranes might afford suitable enclosure. Because the abundance and

genotype distribution of founding populations may be limited (by gut passage in fecal pellets or by bloom dynamics in marine snow), fecal pellets may also encourage the development of solute-trapping microbial associations.

In this study, we predicted that solubilized substrate may be lost from pelagic particle aggregates at rates far exceeding growth requirements of resident microorganisms [15, 47, 74]. Significant fluxes of dissolved OM from marine sediments have also been measured [12]. Widespread excess solubilization generated by cell-free EE may explain not only fluxes of DOM from pelagic aggregates and the seabed, but also the paradox of support for free-living bacteria from OM hydrolysis by particle-attached bacteria in the pelagic ocean. Head-down deposit feeding by many benthic macroorganisms, a counterintuitive feeding strategy due to a general decline in organic richness with increasing depth in the sediment, is another mechanism to exploit DOM released by microbial cell-free EE.

Foraging Distance

Our model findings indicate that the area around the bacterium from which hydrolysate can be collected is limited. We refer to the distance within which 90% of $I_{h,a}$ is produced as the foraging distance. Foraging distance is controlled principally by aggregate diameter and enzyme inactivation rate (Fig. 9; compare predicted foraging distances within and between subplots). In absolute terms, the foraging distance determines the size of the reservoir of potential food that might be exploited. Relative to other bacteria, foraging distance indicates the approximate distance beyond which one cell-free EE forager would not negatively impact another organism. Because hydrolysate from substrate outside the foraging distance is essentially unavailable to the immobilized forager, it cannot successfully compete for this resource.

Predicted foraging distances range from less than 1 to more than 500 μm within the limits of the constant values of Table 1 (Fig. 9). However, all organism-controlled, and most other constants, have opposite effects on foraging distance and $I_{h,a}$. Consequently, the range of foraging distances that might be achieved by a bacterium profitably engaged in cell-free EE foraging is more limited. It probably lies between values obtained with constants at their default settings and those obtained with constants that yield *minimal* foraging distance (and high $I_{h,a}$, where $D_e = 3 \times 10^{-7}$, $\beta = 1000$, $\psi = 0.7$, $\delta = 0.001$, $\phi = 1.8 \times 10^6$, $k_e = 5 \times 10^{-3}$, $\kappa = 100$, $\varepsilon = 0.3$,

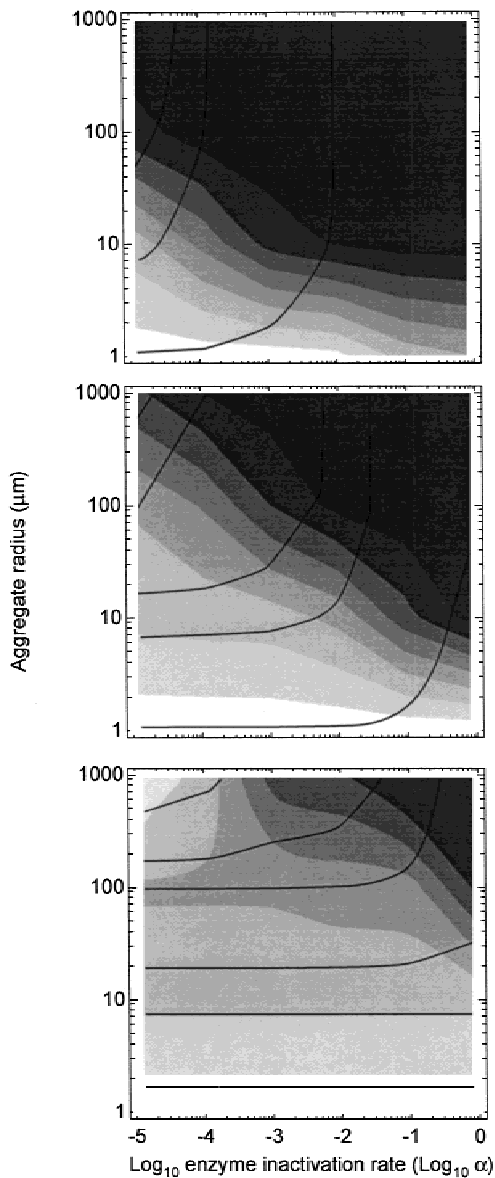


Fig. 9. Distance from within which 90% of hydrolysate current is collected by the cell (foraging distance), as a function of enzyme inactivation rate and aggregate radius. Data generated with constants (Table 1) set at default values (*middle plot*) or to values that yield minimal foraging distance (upper plot: maximal β , ψ , ϕ , k_e , κ , ε , and γ , minimal D_e and δ) or maximal foraging distance (lower plot: maximal D_e and δ ; minimal β , ψ , ϕ , k_e , κ , ε , and γ). Contour lines, increasing from lowest upward, indicate absolute foraging distance of 1, 5, 10, and, where present, 50, 100, and 500 μm . Stippling indicates foraging distance as a percentage of aggregate radius, increasing in isopleths of 10% from darkest (between 10 and 0% of b) to lightest (between 80 and 70% of b).

and $\gamma = 10^{-5}$). For these values, foraging distance is usually L 10 μm . It exceeds 50 μm only for the largest aggregates (and in sediments) and lowest EE inactivation rates, with other constants at their default values.

Because of the restricted upper range of predicted foraging distances, bacteria feeding with cell-free EE and separated by more than 10 μm would not be able to compete with each other by 'stealing' hydrolysate. Each, however, may collect some of the hydrolysate that is inevitably lost by the other due to excess solubilization. The upper boundary on the distance for direct bacterial competition may correspond to an upper boundary on the abundance (volumetric density) of bacteria, beyond which competitive or cooperative interactions between neighboring bacteria are unavoidable. Typical abundances of bacteria in marine sediments ($\sim 10^9$ cells cm^{-3} [25]) do, in fact, correspond to a mean nearest-neighbor distance of 10 μm . Whether bacterial density in sediments and aggregates is related to constraints of cell-free EE feeding is unknown. It may be fruitful to investigate this by examining relationships of bacterial density with bacterial interactions and genotype distributions in environments that support cell-free EE feeding.

Optimal Cell-free EE Release Rates

The enzyme release rate ($I_{e,a}$) is the most conspicuous of the various parameters that the bacterium might adjust to maximize the net benefit (gross energetic benefit–energetic cost) of cell-free EE feeding. $I_{e,a}$ directly reflects energetic cost to the bacterium of cell-free EE feeding; it is also a key determinant of the enzyme concentration at substrate, and, consequently, of the potential energetic benefit of $I_{h,a}$ to the organism. Optimal $I_{e,a}$ is most easily obtained, graphically, by plotting both the gross energetic benefit to the cell ($I_{h,a}$) and the energetic cost to the cell ($I_{e,a} \times \sim 10$; see Appendix D) as a function of the concentration of $I_{e,a}$, and then locating the point at which the positive difference between the two is greatest (Fig. 10). By definition, the cost to the cell must increase linearly with $I_{e,a}$. That the benefit to the cell always increases linearly with $I_{e,a}$ first and then saturates, results from the use of the Langmuir model to describe the substrate-sorbed EE concentration. Optimal $I_{e,a}$ always lies near the top of the benefit function and beyond the linear section, where substrate is becoming saturated with EE and the increase rate of $I_{h,a}$ is decreasing.

For any combination of model constants within the range of values given in Table 1, however, $I_{h,a}$ increases linearly for all $I_{e,a} \leq 10^{-10}$ g s^{-1} (data not shown); $I_{h,a}$ saturates only when $I_{e,a}$ significantly exceeds this value (Fig. 11). Given a linear dependence of $I_{h,a}$ on $I_{e,a}$, the difference between them will be greatest at maximum $I_{e,a}$. Consequently, for any com-

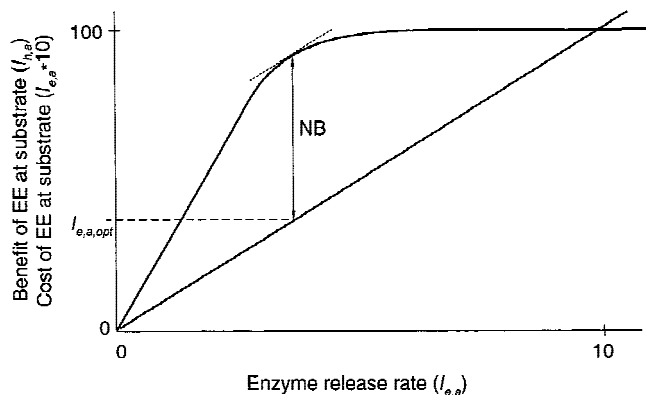


Fig. 10. Optimization of enzyme release rate, which occurs where net benefit is maximized (vertical line with arrow heads). Optimal release rate ($I_{e,a,opt}$) is located by determining where the benefit function (concave-down line) has a slope (dotted line tangent to benefit) equal to the slope of the cost function (straight line intersecting the origin).

bination of constants that may yield net benefit, the predicted optimal EE release rates greatly exceed maximum possible $I_{e,a}$ for any microscopic organism.

This result implies that bacteria feeding by cell-free EE should release EE at a near-maximal rate, the value of which might be determined by optimization with respect to, for example, the kinetics of hydrolysate uptake. Individuals or small groups of bacteria living in porous systems may be expected to manifest a binary cell-free EE feeding mechanism, either producing much cell-free EE or none at all.

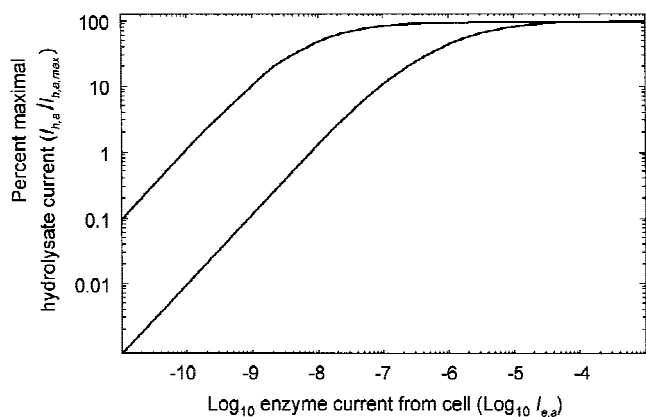


Fig. 11. Percent maximal hydrolysate current as a function of enzyme release rate. Data generated with constants set to default values (lower line) or to values that yield maximum $I_{h,a}$ at lowest $I_{e,a}$ (upper line: maximum k_e , κ , and ψ ; minimum α , ϕ , δ , ϵ , and γ). The increase of $I_{h,a}$ with all $I_{e,a} \leq 10^{-10}$ is essentially linear for all constant values within the ranges given in Table 1.

Exceptions might include individual bacteria using cell-free EE to obtain some limiting micronutrient or to search sediments (see below), and enclosed bacteria, microbial consortia or other systems for which there is a significant background EE concentration or a source of allochthonous DOM.

Active Chemosensing

Cell-free EE concentration near the bacterium can reach $\geq 90\%$ steady state concentration rapidly (Fig. 3). Hydrolysate concentrations around the bacterium stabilize at least as quickly as EE concentrations once hydrolysis rates (EE concentrations) are stable (molecular weights of hydrolysates are lower than those of EE and predicted diffusivities correspondingly higher). Thus, the concentration of hydrolysate at the cell surface after twice the time required for cell-free EE concentrations to approach steady state at distance r from the bacterium (the time for the round trip of EE from the cell surface to particle-sorbed OM and of hydrolysate from the particle back to the bacterium) is an indicator of the potential rate of hydrolysate collection from substrates within r . By sensing the change in the hydrolysate concentration at its cell surface the bacterium might “search” sediment by “active chemosensing.”

This “active chemosensing” search rate can be estimated conservatively as (sediment volume within r)/(twice time to approach steady state at r). For $r = 5 \mu\text{m}$, the rate is between $10^{-13} \text{ cm}^3 \text{ s}^{-1}$ (default values) and $10^{-10} \text{ cm}^3 \text{ s}^{-1}$ (large a , α ; small ψ), increasing approximately linearly with search radius. These conservative estimates of search rates by “active chemosensing” are comparable to, or in excess of, generous estimates of search rates by direct contact. For example, a bacterium of $0.5\text{-}\mu\text{m}$ radius gliding at $2 \mu\text{m s}^{-1}$ and contacting sediment on all of its volume-specific surface area of $30 \text{ m}^2 \text{ cm}^{-3}$ contacts particle surfaces at a rate of $2.1 \times 10^{-13} \text{ cm}^3 \text{ s}^{-1}$.

In addition to the potential to greatly increase sediment search rates, active chemosensing using cell-free EE may offer other advantages by interaction of cell surface and substrate. Cell-free EE can reach substrates that may be physically isolated from the organism. By obviating the need for much cell movement, active chemosensing may reduce encounter with predators. Because the rate at which cell-free EE concentration approaches steady state is independent of $I_{e,a}$ (eq. A2), relatively little EE may be needed for active chemosensing. Active chemosensing may thus be a useful foraging strategy, even in environments where cell-free EE

feeding is not; EE may be released at a low rate to rapidly locate substrate that might be collected with greatest net gain by passive absorption or with the activity of cell-attached enzymes.

The chemosensing benefits of cell-free EE may extend to macroorganisms. Elevated EE activity is associated with the appendages of some deposit feeders [53]. EE released into particles upon initial contact with macrofaunal feeding appendages may generate sufficient hydrolysate during particle handling for detection by sensors near the animal's mouth. The particle might then be ingested or rejected based on the potential, inferred from this "taste," for further hydrolysate production during gut passage.

Other Systems

Systems in which diffusive loss of EE or excess solubilization is reduced may support cell-free EE feeding at least as well as porous aggregates and sediments. Foraging by microbial consortia, channeling by exopolymer, and enclosure within fecal pellets (discussed above) may decrease losses of EE and hydrolysate. Microtopography and surfaces can also constrain diffusion, reducing effective dimensionality and increasing the geometry-dependent fraction of diffusively transported hydrolysate collected by the forager. Surfaces may reduce solute loss from biofilm-forming organisms by decreasing the resources required to enclose substrate or recapture hydrolysate downstream in flowing liquids. These mechanisms to enhance cell-free EE foraging may be particularly important for microbial growth in energetic environments, such as stream and river beds, and the marine intertidal, as well as on surfaces of aquatic animals and implants in living organisms such as medical catheters. Microorganisms such as fungi, with morphologies more complex than bacteria, may be able to effect partial enclosure independent of mutualism or surface effects. The unique degradative capabilities of some fungi (e.g. lignin and chlorinated organics) may result from this ability. Nearly complete enclosure of cell-free EE-producing bacteria within guts or between carapace and soft tissues of some organisms, such as crabs, may dramatically reduce solute loss. The evolution of digestive associations of microorganisms and multicellular animals (e.g., cows or termites) may stem in part from the potential for both host and symbiont to benefit by sharing hydrolysate that would otherwise be lost from the isolated EE forager due to excess solubilization. These and other systems could be modeled with eqs. 1 and 2 by appropriate

replacement of the diffusion terms or substitution of flux boundary conditions at b .

Conclusions

The dynamic world in which microorganisms live is vastly more complicated than the simple model described here. Wherever possible, however, simplifications were chosen to yield conservative estimates of potential benefits from cell-free EE foraging, to broaden the scope of application, and to ensure that important model conclusions are robust.

From this initial modeling effort, we can predict that cell-free EE foraging should be a powerful bacterial feeding mechanism in high-surface-area, organic-rich, liquid-bathed environments, with the potential to support maximal growth rates. Where net energetic gain is the purpose of producing cell-free EE, bacteria can be expected to release enzymes at high rates. Excess solubilization of POM, and consequent large DOM fluxes away from sites of active hydrolysis, appear to be necessary outcomes of diffusive solute transport during cell-free EE feeding. The distance from which enzymatic hydrolysate may be effectively collected is similarly limited, with important implications for the establishment of mutualisms and consortia. Further advantage can be gained from cell-free EE feeding, and the range of suitable systems significantly extended, by various mechanisms for reducing diffusive solute loss. Many organisms may use cell-free EE to search for food, even in environments in which actual feeding is optimized by some other mechanism.

Bacterial EE play a central part in the microbiology, biogeochemistry, and ecology of the sea, by virtue of their abundance, ubiquity, and broad activity ranges. Our model predictions indicate that cell-free EE, in particular, may occupy a central role in these processes, due to their likely concentration at sites of high productivity and OM flux, disproportionate effects on material transformations, and enhanced potential for engendering micro- and macrobiological interactions.

Acknowledgments

This research was supported by ONR grants to JWD and PAJ, and by the ONR-supported Marine Bioremediation

Program at the University of Washington. We thank Paul Hill and two anonymous reviewers for their helpful input.

References

1. Alldredge AL, Cole JJ, Caron DA (1986) Production of heterotrophic bacteria inhabiting organic aggregates (marine snow) from surface waters. *Limnol Oceanogr* 31:68–78
2. Alldredge AL, Passow U, Logan BE (1995) The abundance and significance of a class of large, transparent organic particles in the ocean. *Deep-Sea Res I* 40:1131–1140
3. Almeida MA, Alcantara F (1992) Bacterial colonization of seston particles in brackish waters (Ria de Aveiro, Portugal). *Mar Ecol Prog Ser* 89:165–173
4. Ammerman JW, Azam F (1985) Bacterial 5'-nucleotidase in aquatic ecosystems: a novel mechanism of phosphorus regeneration. *Science* 277:1338–1340
5. Beguin P, Eisen H, Roupas A (1977) Free and cellulose-bound cellulases in a *Cellulomonas* sp. *J Gen Microbiol* 101:191–196
6. Bell CR, Albright LJ (1981) Attached and free floating bacteria in the Fraser River estuary, British Columbia, Canada. *Mar Ecol Prog Ser* 6:317–327
7. Benner R, Moran MA, Hodson RE (1986) Biogeochemical cycling of lignocellulosic carbon in marine and freshwater ecosystems: Relative contributions of procaryotes and eucaryotes. *Limnol Oceanogr* 31:89–100
8. Berg HC (1983) *Random Walks in Biology*. Princeton University Press, New Jersey
9. Berg HC, Purcell EM (1977) Physics of chemoreception. *Biophys J* 20:193–215
10. Boto KG, Alongi DM, Nott ALJ (1989) Dissolved organic carbon-bacteria interactions at sediment-water interface in a tropical mangrove system. *Mar Ecol Prog Ser* 51:243–251
11. Bowen JD, Stolzenbach KD, Chisholm SW (1994) Simulating bacterial clustering around phytoplankton cells in a turbulent ocean. *Limnol Oceanogr* 38:36–5
12. Burdige DJ, Alperin MJ, Homstead J, Martens SM (1992) The role of benthic fluxes of dissolved organic carbon in oceanic and sedimentary carbon cycling. *Geophys Res Lett* 19:1851–1854
13. Button DK (1993) Nutrient-limited microbial growth kinetics: overview and recent advances. *Antonie Van Leeuwenhoek* 63:225–235
14. Cammen LM, Walker JA (1982) Distribution and activity of attached and free-living suspended bacteria in the Bay of Fundy. *Can J Fish Aquatic Sci* 39:1655–1663
15. Cho BC, Azam F (1988) Major role of bacteria in biogeochemical fluxes in the ocean's interior. *Nature* 332:441–443
16. Chróst RJ, Rai H (1993) Ecto-enzyme activity and bacterial secondary production in nutrient-impooverished and nutrient-enriched mesocosms. *Microb Ecol* 25:131–150
17. Cohen D, Parnas H (1976) An optimal policy for the metabolism of storage materials in unicellular algae. *J Theoret Biol* 56:1–18
18. Constantino HR, Brown SH, Kelley RM (1990) Purification and characterization of an alpha-glucosidase from a hyperthermophilic archaeobacterium *Pyrococcus furiosus* exhibiting temperature optimum of 105 to 115 degrees C. *J Bacteriol* 172:3654–3660
19. Corpe WA, Winters H (1972) Hydrolytic enzymes of some periphytic marine bacteria. *Can J Microbiol* 18:1483–1490
20. Costerton JW, Cheng KJ, Geesey GG, Ladd TI, Nickel JC, Dasgupta M, Marrie TJ (1987) Bacterial biofilms in nature and disease. *Ann Rev Microbiol* 41:435–464
21. Crank J (1975) *The Mathematics of Diffusion*. Oxford University Press, New York
22. Cussler EL (1984) *Diffusion: Mass Transfer in Fluid Systems*. Cambridge University Press, New York
23. DeLong EF, Franks DG, Alldredge AL (1993) Phylogenetic diversity of aggregate-attached vs. free-living marine bacterial assemblages. *Limnol Oceanogr* 38:924–934
24. Deming JD, Baross JA (1993) The early diagenesis of organic matter: Bacterial activity. In: Engel MH and Macko SA (eds) *Organic Geochemistry*. Plenum Press, New York
25. Deming JD, Yager PY (1992) Natural bacterial assemblages in deep-sea sediments: towards a global view. In: Rowe GT, Pariente V (eds) *Deep-Sea Food Chains and the Global Carbon Cycle*. Kluwer Academic, The Netherlands
26. Dijkerman R, Vervuren MBF, Op den Camp HJM, Van der Drift C (1996) Adsorption characteristics of cellulolytic enzymes from the anaerobic fungus *Piromyces* sp strain E2 on microcrystalline cellulose. *Appl Environ Microbiol* 62:20–25
27. Ferreira LMA, Durant AJ, Hall J, Hazelwood GP, Gilbert HJ (1990) Spatial separation of protein domains is not essential for catalytic activity or substrate binding in a xylanase. *Biochem J* 269:261–264
28. Fowler SW, Knauer GA (1986) Role of large particles in the transport of elements and organic compounds through the oceanic water column. *Prog Oceanogr* 16:147–194
29. Geesey GG, White DC (1990) Determination of bacterial growth and activity at solid-liquid interfaces. *Ann Rev Microbiol* 44:579–602
30. Gottschalk G (1992) *Bacterial Metabolism*. Springer-Verlag, New York
31. Grant WD, Atkinson M, Burke B, Molloy C (1996) Chitinolysis by the marine ascomycete *Colorollospora maritime* Werdermann: purification and properties of a chitobiosidase. *Botanica Marina* 39:177–186
32. Griffin HL, Freer SN, Green RV (1987) Extracellular endoglucanase activity by a novel bacterium isolated from marine shipworm. *Biochem Biophys Res Comm* 144:143–151
33. Harms H, Zehnder AJB (1994) Influence of substrate diffusion on degradation of dibenzofuran and 3-chlorodibenzofuran by attached and suspended bacteria. *Appl Environ Microbiol* 60:2736–2745
34. Harvey HW (1925) Oxidation in seawater. *J Mar Biol Assoc United Kingdom* 18:953–969

35. Herndl GJ, Peduzzi P, Fanuko N (1989) Benthic community metabolism and microbial dynamics in the Gulf of Trieste (northern Adriatic Sea). *Mar Ecol Prog Ser* 53:169–178
36. Hodson RE, Maccubbin AE, Pomeroy LR (1981) Dissolved adenosine triphosphate utilization by free-living and attached bacterioplankton. *Mar Biol* 64:43–61
37. Hollibaugh JT, Azam F (1983) Microbial degradation of dissolved proteins in seawater. *Limnol Oceanogr* 28:1104–1116
38. Hoppe HG (1983) Significance of exoenzymatic activities in the ecology of brackish water: measurements by means of methylumbelliferyl-substrates. *Mar Ecol Prog Ser* 11:299–308
39. Hoppe HG, Ducklow H, Karrasch B (1993) Evidence for dependency of bacterial growth of enzyme hydrolysis of particulate organic matter in the mesopelagic ocean. *Mar Ecol Prog Ser* 93:277–283
40. Imam SH, Greene RV, Griffin HL (1993) Binding of extracellular carboxymethylcellulose activity from the marine shipworm bacterium to insoluble cellulosic substrates. *Appl Environ Microbiol* 59:1259–1263
41. Jackson A (1989) Simulation of bacterial attraction and adhesion to falling particles in an aquatic environment. *Limnol Oceanogr* 34:514–530
42. Jones JG (1971) Studies on freshwater bacteria: factors which influence the population and its activity. *J Ecol* 59:593–613
43. Jumars PA (1993) *Concepts in Biological Oceanography*. Oxford University Press, New York
44. Jumars PA, Penry DL, Baross JA, Perry MJ, Frost BW (1989) Closing the microbial loop: Dissolved carbon pathway to heterotrophic bacteria from incomplete digestion and adsorption in animals. *Deep-Sea Res* 36:483–495
45. Jumars PA, Deming JW, Hill PS, Karp-Boss L, Yager PL (1993) Physical constraints on marine osmotrophy in an optimal foraging context. *Mar Microb Foods Webs* 7:121–159
46. Kadowaki T, Yoneda M, Okamoto K, Naeda K, Yamamoto K (1994) Purification and characterization of a novel arginine-specific cysteine protease (argigipain) involved in the pathogenesis of periodontal disease from the culture supernatant of *Porphyromonas gingivalis*. *J Biol Chem* 269:21371–21378
47. Karner M, Herndl GJ (1992) Extracellular enzymatic activity and secondary production in free-living and marine-snow-associated bacteria. *Mar Biol* 113:341–347
48. Karner M, Rassoulzadegan F (1995) Extracellular enzyme activity: indications for high short-term variability in a coastal marine ecosystem. *Microb Ecol* 30:143–156
49. Karp-Boss L, Boss E, Jumars PA (1996) Nutrient transfer to planktonic osmotrophs in the presence of fluid motion. *Oceanogr Mar Biol Annu Rev* 34:71–107
50. Keil RG, Tsamakis E, Fuh CB, Giddings JC, Hedges JJ (1993) Mineralogical and textural controls on the organic composition of coastal marine sediments: hydrodynamic separation using SPLITT-fractionation. *Geochim Cosmochim Acta* 57:879–893
51. Klibanov AM (1983) Approaches to enzyme stabilization. *Biochem Soc Trans* 11:19–20
52. Koch AL (1985) The macroeconomics of bacterial growth. In: Fletcher M, Floodgate GD (eds) *Bacteria in Their Natural Environments*. Academic Press, London
53. Koster M, Meyer-Reil LA (1994) Hydrolytic activity associated with organisms and biogenic structures in deep-sea sediments. In: Chrost R (ed) *Microbial enzymes in aquatic environments*. Springer Verlag, NY
54. Krepps E (1934) Organic catalysts or enzymes in the sea. In: James Johnstone Memorial Volume, University Press, Liverpool
55. Mathews CK, van Holde KE (1990) *Biochemistry*. Benjamin/Cummings Publishing Co., Redwood City, CA
56. Mayer LM (1994) Relationships between mineral surfaces and organic matter concentrations in soils and sediments. *Chem Geol* 114:347–363
57. Mayer LM, Schick LL, Sawyer T, Plante CJ, Jumars PA, Self RL (1995) Bioavailable amino acids in sediments: A biomimetic, kinetics-based approach. *Limnol Oceanogr* 40:511–520
58. McMeekin TA, Olley J, Ratkowsky DA (1988) Temperature effects on microbial growth rates. In: Bazin MJ, Prosser JI (eds) *Physiological Models in Microbiology*. CRC Press, Boca Raton
59. Moriarty DJW, Hayward AC (1982) Ultrastructure of bacteria and the proportion of gram-negative bacteria in marine sediments. *Microb Ecol* 8:1–14
60. Nagata T, Kirchman DL (1992) Release of macromolecular organic complexes by heterotrophic marine flagellates. *Mar Ecol Prog Ser* 83:233–240
61. Ofek I, Doyle RJ (1994) *Bacterial Adhesion to Cells and Tissues*. Chapman and Hall, New York
62. Overbeck J (1991) Early studies on ecto- and extracellular enzymes. In: Chróst RJ (ed) *Microbial Enzymes in Aquatic Environments*. Springer-Verlag, New York
63. Paerl HW, Pinckney JL (1996) A mini review of microbial consortia: their roles in aquatic production and biogeochemical cycling. *Microb Ecol* 31:225–247
64. Parnas H, Cohen D (1976) The optimal strategy for the metabolism of reserve materials in microorganisms. *J Theoret Biol* 56:19–55
65. Pedros-Alio C, Brock TD (1983) The importance of attachment to particles for planktonic bacteria. *Arch Hydrobiol* 98:354–379
66. Plante CJ, Jumars PA, Baross JA (1990) Digestive associations between marine detritivores and bacteria. *Annu Rev Ecol Sys* 21:93–127
67. Pomeroy LR, Weibe WJ (1993) Energy sources for microbial food webs. *Mar Microb Food Webs* 7:101–118
68. Rego JV, Billen G, Fontigny A, Someville M (1985) Free and attached proteolytic activity in water environments. *Mar Ecol Prog Ser* 21:245–249
69. Rheinheimer G (1992) *Aquatic Microbiology*. John Wiley and Sons, West Sussex, UK
70. Sander BC, Kalf J (1993) Factors controlling bacterial production in marine and freshwater sediments. *Microb Ecol* 26:79–99

71. Schuster GS (1990) Oral Microbiology and Infectious Disease. BC Becker, Philadelphia
72. Scholz B, Boon PI (1993) Biofilm development and extracellular enzyme activities on wood in billabongs of south-eastern Australia. *Freshwat Biol* 30:359–368
73. Simpson WR (1982) Particulate matter in the oceans—sampling methods, concentration, size distribution and particle dynamics. *Oceanogr Mar Biol Ann Rev* 20:119–172
74. Smith DC, Simon M, Alldredge AL, Azam F (1992) Intense hydrolytic activity on marine aggregates and implications for rapid particle dissolution. *Nature* 359:139–142
75. Someville M, Billen G (1983) A method for determining exo-proteolytic activity in natural waters. *Limnol Oceanogr* 28:190–193
76. Stolzenbach KD (1993) Scavenging of small particles by fast-sinking porous aggregates. *Deep-Sea Res* 40:359–369
77. Sugita H, Tanaami H, Deguchi Y (1982) Measurement of the bacterial count in the sediments with Gram staining method. *Bull Jap Soc Fish* 48:1469–1471
78. Sweerts J-PRA, Kelly CA, Rudd JWM, Hesslein R, Capenberg TE (1991) Similarity of whole-sediment diffusion coefficients in freshwater sediments of low and high porosity. *Limnol Oceanogr* 36:335–342
79. Takeuchi JI, Hata Y (1985) Distribution of bacteria associated with various sizes of particulate matter in Harima-Nada and Hiuchi-Nada areas, Seto inland Sea, Japan. *Jap J Ecol* 35:49–56
80. Tomazic SJ (1991) Protein stabilization. In: *Biocatalysts for Industry*. Plenum Press, New York
81. Tomazic SJ, Klivanov AM (1988) Mechanisms of irreversible thermal inactivation of *Bacillus* alpha-amylases. *J Biol Chem* 263:3086–91
82. Tramper J (1994) Applied biocatalysis: from product request to idea to product. In: *Applied Biocatalysis*. Harwood Academic Publishing, Chur, Switzerland
83. Trick CG (1989) Hydroxamate-siderophore production and utilization by marine eubacteria. *Curr Microbiol* 18:375–378
84. Unanue M, Azua I, Barcina I, Egea L, Iriberrri J (1993) The size distribution of aminopeptidase activity and bacterial incorporation of dissolved substrates in three aquatic ecosystems. *FEMS Microb Ecol* 102:175–183
85. van Loosdrecht MCM, Lyklema J, Norde W, Zehnder AJB (1990) Influence of interfaces on microbial activity. *Microbiol Rev* 54:75–87
86. van den Tweel WJJ, Leak D, Bielecki S, Pedersen S (1994) Biocatalyst production. In: *Applied Biocatalysis*. Harwood Academic Publishing, Chur, Switzerland
87. Weise W, Rheinheimer G (1978) Scanning electron microscopy and epifluorescence investigation of bacterial colonization of marine sand sediments. *Microb Ecol* 4:175–188
88. Weiss MS, Abele U, Weckesser J, Welte W, Schlitz E, Schultz GE (1991) Molecular architecture and electrostatic properties of a bacterial porin. *Science* 254:1627–1630
89. Wimpenny JWT, Colasanti R (1997) A unifying hypothesis for the structure of microbial biofilms based on cellular automation models. *FEMS Microbiol Ecol* 22:1–16

Appendices

Appendix A. Solute Diffusion in a Porous Aggregate

The porous aggregate used in this modeling effort is characterized by pore diameters significantly larger than diffusional step lengths and porosities greater than the percolation threshold. Under these circumstances, the procedure used by Berg [8] to derive Fick's first law can be used without modification. The result is identical to the case without particles:

$$J = \left(-D \frac{\partial}{\partial r} C \right)$$

where J and C are the solute flux and concentration, respectively, in liquid only. Thus, for diffusion in pore water, the solid volume fraction ψ affects only the total current (flux times area) of solute:

$$I = J(1 - \psi)4\pi r^2$$

The procedure used by Crank [21] to derive Fick's second law can be used if concentration terms for liquid and surface-sorbed phases are separated and fluxes are summed over the pore water area, only. Consider solute concentrations and fluxes in a spherical shell of radius r and thickness Δr . Particles fill a fraction of the shell volume ψ , liquid fills the remaining fraction, $1 - \psi$. Solute diffusion occurs in liquid, only. The total amount of solute in the shell is:

$$(C(1 - \psi) + Ck\psi)4\pi r^2 \Delta r$$

where C is the solute concentration in pore water (g cm^{-3}) and k is the coefficient for solute partition between liquid and particle ($\text{g (particle volume)}^{-1}$: $\text{g (liquid volume)}^{-1}$). The diffusion current into the shell is:

$$I_{in} = J4\pi r^2 |_{r-} (1 - \psi);$$

the current out of the shell is:

$$I_{out} = J4\pi r^2 |_{r+\Delta r} (1 - \psi).$$

The change rate of total solute in the shell ($I_{in} - I_{out}$) is:

$$\frac{\partial}{\partial t} (C(1 - \psi) + Ck\psi)4\pi r^2 \Delta r = I_{in} - I_{out} = J4\pi r^2 |_{r-} (1 - \psi) - J4\pi r^2 |_{r+\Delta r} (1 - \psi),$$

and the change rate of concentration is

$$\frac{\partial}{\partial t} (C(1 - \psi) + Ck\psi) \equiv \left(\frac{1 - \psi}{r^2} \right) \frac{J|_{r-} r^2 - J|_{r+\Delta r} (r + \Delta r)^2}{\Delta r}.$$

By the definition of the derivative, as $\Delta r \rightarrow 0$,

$$\frac{\partial}{\partial t} (C(1 - \psi) + Ck\psi) = \left(\frac{1 - \psi}{r^2} \right) \frac{\partial}{\partial r} (Jr^2) = D \left(\frac{1 - \psi}{r^2} \right) \frac{\partial}{\partial r} \left(r^2 \frac{\partial}{\partial r} C \right).$$

Taking the derivative, with respect to r , then:

$$\frac{\partial}{\partial t} (C(1 - \psi) + Ck\psi) = D(1 - \psi) \left(\frac{\partial^2}{\partial r^2} C + \frac{2}{r} \frac{\partial}{\partial r} C \right).$$

Appendix B. Analytical Concentration Equations

An analytical solution for the solute concentration around a spherical continuous source approximating solutions obtained with eq. 1 can be found by assuming that:

- (1) equilibrium between solute concentrations in dissolved and sorbed phases is reached much faster than steady-state concentrations, overall, so that concentrations in each phase reach steady state at the same rate; and
- (2) dissolved enzyme concentrations are well below substrate-saturating levels, so the concentration of substrate-sorbed enzyme, $C_d/(C_e + 1/k_e\kappa \phi \varepsilon \delta \gamma)$, can be approximated as $C_e \phi \varepsilon \delta \gamma k_e \kappa$.

Eq. 1 can then be rewritten:

$$\frac{\partial}{\partial t} C_e = (1 - \psi) \frac{D_e}{K_1} \left(\frac{2}{r} \frac{\partial}{\partial r} C_e + \frac{\partial^2}{\partial r^2} C_e \right) - \alpha C_e$$

where $K_1 = (1 - \psi) + (1 - \delta) \psi \phi k_e + \phi \varepsilon \delta \gamma k_e \kappa$. A general solution to this equation, describing the concentration at radius r and time t after a single instantaneous release of solute, is:

$$C_e(r, t) = A t^{-(3/2)} e^{-(r^2/(4K_2t) + \alpha t)}$$

where K_2 stands for $(1 - \psi)D_e/K_1$ and A is an arbitrary constant. A can be expressed in terms of the total amount of solute released instantaneously M_0 , noting that, at any time after solute release, the total amount of solute remaining, M , has decreased exponentially due to enzyme inactivation at the rate α . The total amount of enzyme present at time t is, therefore:

$$M_0 e^{-\alpha t} = \int_0^\infty C_e dr.$$

Solving for A and substituting into the expression for C_e above gives:

$$C_e(r, t) = \frac{M_0}{8(D_e \pi t)^{3/2}} e^{-(r^2/(4K_2t) + \alpha t)}.$$

The solution for the concentration due to a continuous source is obtained by integrating C_e over time, noting that, over each time interval dt , the total amount of solute released is $I_{e,a} dt$, where $I_{e,a}$ is the constant rate at which solute is released from a . The time-dependent enzyme concentration due to a continuous enzyme source with enzyme inactivation is then:

$$C_e(r, t) = \frac{I_{e,a}}{8(D_e \pi)^{3/2}} \int_0^t (t - t')^{-3/2} e^{-(r^2/(4K_2(t-t')) + \alpha(t-t'))} dt'. \quad (A1)$$

We know of no general analytical solution for this equation.

For the case of no enzyme inactivation ($\alpha = 0$), however, an analytical solution for eq. A1 does exist:

$$C_e(r, t) = \frac{I_{e,a}}{4\pi K_2 r} \operatorname{erfc} \left(\frac{r-a}{\sqrt{4K_2 t}} \right) \quad (A2)$$

where boundary conditions are enzyme release rate = I_e at $r = a$ and enzyme concentration $C_e = 0$ at $r = \infty$. It can be seen numerically that this is a conservative (biased long) estimate of the rate at which steady-state concentration is reached around a continuous source

with inactivation: diffusion removes solute; enzyme inactivation is also effectively a solute removal process; and, steady-state occurs faster with faster diffusion and inactivation.

Similarly, at steady state (and with enzyme inactivation) an analytical solution for eq. A1 also exists:

$$C_e(r) = \frac{I_{e,a}}{4\pi K_2 r} \left(\frac{e^{(a-r)\sqrt{\alpha/K_2}}}{1 + a\sqrt{\alpha/K_2}} \right) \quad (A3)$$

where boundary conditions are again enzyme release rate = I_e at $r = a$ and enzyme concentration $C_e = 0$ at $r = \infty$.

Appendix C. Estimated Time to Substrate Exhaustion by a Bacterium in a Marine Sediment

The time at which all substrate available to a cell-free EE-foraging bacterium will have been consumed can be estimated from bacterial growth and substrate availability data as (time to substrate exhaustion) = (sediment OC content \times reservoir volume from which hydrolysate is produced \times fraction of solute collected \times bacterial growth efficiency)/(bacterial growth rate \times C content of bacterium).

A conservative (biased short) estimate can be made by assuming:

- (1) low sediment OC content (0.01 g C cm⁻³);
- (2) small reservoir volume (short foraging distance; sphere of 5 μ m radius);
- (3) moderate fractional hydrolysate collection (0.05; Fig. 8);
- (4) low bacterial growth efficiency (0.05);
- (5) high in situ growth rate (0.1 d⁻¹ [70]);
- (6) high bacterial C content (2×10^{-14} g C bacterium⁻¹; twice the value in [25]).

With these figures, more than 3 h pass before substrate exhaustion. In many cases, time to exhaustion is probably much longer: in large aggregates where foraging distances may be greater; in rich micro-zones where local OC content is higher; at low temperatures where growth rates are reduced; in enclosures or within consortia where fractional hydrolysate collection is higher (see text), and where episodic advection renews the supply.

Appendix D. Relative Value of Hydrolysate and Cell-free EE

The relative value of hydrolysate and cell-free EE, assuming roughly equal value of constituent amino acids, depends on the value added to collected hydrolysate during cell-free EE synthesis by the cell. Value is added to collected hydrolysate as the cell expends metabolic energy and consumes chemical resources to decompose hydrolysate and synthesize EE, as well as during intracellular and transmembrane transport of hydrolysate, cell-free EE, and intermediaries. Value added is poorly constrained. Bacterial gross growth efficiencies can be interpreted as value added to average growth substrate integrated over the whole lifetime of the organism, and the entirety of its metabolic and other processes, including, but not limited to, cell-free EE feeding. On this basis, a 'typical'

bacterial growth efficiency of about 10% [67] corresponds to 10-fold value added. Relative values can also be estimated from energy balances for protein synthesis. This approach may be appropriate, because both cell-free EE and important natural substrates are polypeptides. In *Escherichia coli*, polymerization of amino acids to form proteins (presumably including cell-free EE) consumes between 4 and 13 times as much energy as does *de novo* production of amino acids [30]. This multiplier corresponds to the value added

to amino acids returned to the cell (i.e. proteinaceous hydrolysate), compared to amino acids exported from the cell (i.e. cell-free EE). This estimate does not include energy for hydrolysate decomposition prior to protein polymerization, or for trans-membrane transport. We use a ratio of 1:10 for the relative values for the same weight of hydrolysate and cell-free EE, recognizing that the true value probably varies widely among substrates, enzymes, and, perhaps, organisms.